

UCSF

UC San Francisco Previously Published Works

Title

Distinct Luminal-Type Mammary Carcinomas Arise from Orthotopic Trp53-Null Mammary Transplantation of Juvenile versus Adult Mice

Permalink

<https://escholarship.org/uc/item/8np1q98k>

Journal

Cancer Research, 74(23)

ISSN

0008-5472

Authors

Nguyen, David H
Ouyang, Haoxu
Mao, Jian-Hua
[et al.](#)

Publication Date

2014-12-01

DOI

10.1158/0008-5472.can-14-1440

Peer reviewed



Published in final edited form as:

Cancer Res. 2014 December 1; 74(23): 7149–7158. doi:10.1158/0008-5472.CAN-14-1440.

Distinct luminal type mammary carcinomas arise from orthotopic *Trp53* null mammary transplantation of juvenile versus adult mice

David H. Nguyen¹, Haoxu Ouyang¹, Jian-Hua Mao², Lynn Hlatky³, and Mary Helen Barcellos-Hoff^{1,4}

David H. Nguyen: d.hh.nguyen@gmail.com; Haoxu Ouyang: haoxu.ouyang@nyumc.org; Jian-Hua Mao: jhmao@lbl.gov; Lynn Hlatky: lynn.hlatky@tufts.edu

¹Department of Radiation Oncology, New York University School of Medicine, New York, NY, 10016, USA

²Life Sciences Division, Lawrence Berkeley National Laboratory, Berkeley CA, 94705 USA

³Center of Cancer Systems Biology, GeneSys Research Institute, Tufts University School of Medicine, St. Elizabeth's Medical Center, Boston, MA, 02135 USA

Abstract

Age and physiological status, like menopause, are risk factors for breast cancer. Less clear is what factors influence the diversity of breast cancer. In this study, we investigated the effect of host age on the distribution of tumor subtypes in mouse mammary chimera consisting of wild-type hosts and *Trp53* nullizygous epithelium, which undergoes a high rate of neoplastic transformation. Wild-type mammary glands cleared of endogenous epithelium at 3 weeks of age were subsequently implanted during puberty (5 weeks) or at maturation (10 weeks) with syngeneic *Trp53* null mammary tissue fragments and monitored for 1 year. Tumors arose sooner from adult hosts (AH) compared to juvenile hosts (JH). However, compared to AH tumors, JH tumors grew several times faster, were more perfused, exhibited a 2-fold higher mitotic index and were more highly positive for insulin-like growth factor receptor phosphorylation. Most tumors in each setting were ER positive (80% JH vs 70% AH) but JH tumors were significantly more ER immunoreactive ($p=0.0001$) than AH tumors. A differential expression signature (JvA) of juvenile versus adult tumors revealed a luminal transcriptional program. Centroids of the human homologs of JvA genes showed that JH tumors were more like luminal A tumors and AH tumors were more like luminal B tumors. Hierarchical clustering with the JvA human ortholog gene list segregated luminal A and luminal B breast cancers across data sets. These data support the notion that age-associated host physiology greatly influences the intrinsic subtype of breast cancer.

⁴**Corresponding Author:** Mary Helen Barcellos-Hoff, Department of Radiation Oncology, New York University, School of Medicine, 566 First Avenue, New York, NY 10016, Phone: 212-263-3021, Fax: 212-263-6274, mhbarcellos-hoff@nyumc.org.

Authors Contributions: DHHN conducted the experiments, analyzed the data and prepared the figures and draft manuscript; HO analyzed the data and prepared the figures and draft manuscript; LH advised on microarray analysis and JHM supervised experiments and analysis; MHBH designed the experiment, supervised the research, analyzed the data and wrote the manuscript.

Competing Interest

D.H. Nguyen serves as a consultant to Creative Bioninformatics Consulting and is Editor-in-Chief for *Cancer InCytes* magazine. The other authors declare that they have no competing interests.

Keywords

puberty; breast cancer; intrinsic breast cancer subtypes; etiology; Trp53; IGF1

Introduction

Breast cancer is a heterogeneous disease, or rather, a collection of neoplastic diseases. As tumor characteristics are highly correlated with prognosis, there has been considerable investment in defining classes and standardizing the characterization of breast tumors based on traditional pathology, marker analysis, imaging features and molecular analysis. Human epidermal growth factor receptor 2 (HER2) amplification distinguishes a specific breast cancer subtype that provides a robust molecular target in therapy (1). Estrogen receptor (ER) status is important not only because ER-positive tumors are managed with anti-estrogen treatments but also because ER status is with different age groups and with different outcomes. ER-negative tumors are more frequent in young women and have a worse prognosis (2). Among ER-negative breast cancers there are also several diseases. ER- and progesterone receptor (PR)-negative cancers tend to be poorly differentiated and aggressive. Triple-negative breast cancer that lack both hormone receptors and HER2 amplification are usually invasive ductal carcinomas that have a high rate of relapse (3).

Molecular profiling discriminates between 5 and 20 tumor types depending on the algorithms and datasets employed (reviewed in (4)). As defined by Perou, transcriptomic analysis of human breast cancer comprises at least six different intrinsic molecular subtypes: luminal-A, luminal-B, HER2, basal-like, claudin-low, and normal-like (5–7). Molecular classification is not synonymous with clinical marker status using ER, PR and HER2. For example, although ER-positive tumors predominate in post-menopausal women and have a relatively low relapse rate, molecular characterization revealed that ER-positive breast cancers can be divided into the so-called luminal A cancers, which are associated with a longer disease-free survival than that of luminal B cancers. The luminal A and B subtypes are known to maintain the expression of *ESR1* transcript and protein, along with the canonical mammary luminal fate regulators *GATA3* and *FOXA1* (8,9), but the luminal B subtype has a strong signature of proliferation.

While tumor characteristics are clearly linked with prognosis, it is less clear how these distinct features arise. One source of biological distinction between breast tumors is thought to be the cell of origin at transformation (10). A “cells of origin” autonomous view of breast cancer is bolstered by several studies in which disruption of the progenitor fate regulator, *BRCA1*, via promoters specific to the basal mammary gland compartment, produced tumors that resembled human basal-like breast cancers (11–13). Alternatively, deregulation of key transcriptional regulator, whether by mutation or epigenetic alteration, may divert cells to a particular state. For example, Gata3, a necessary transcriptional factor for differentiation of luminal cells, is associated with the luminal subtype of breast cancers (14–16). External factors are suggested by epidemiological studies of girls exposed to ionizing radiation, who develop triple-negative breast cancer at an early age (17,18), and the association of specific tumor types with obesity (19). Several recent studies have turned attention on the stroma to

derive prognostic value by using expression profiling of stromal and extratumoral tissues (20). Using microdissected stroma from breast cancer, Finak et al. found a stroma-derived prognostic predictor that stratifies disease outcome based on a signature of immune mediators, hypoxia and angiogenesis (21). Analysis of the expression profiles from invasive breast cancer and ductal carcinoma *in situ* provides evidence that stromal biology is a key determinant of progression (22). Consistent with the influence of distinct microenvironment subtypes, an active versus inactive cancer-adjacent microenvironment is associated with aggressiveness and outcome of ER-positive human breast cancers (20).

The stromal factors that contribute to breast cancer subtype distribution are not mutually exclusive and may be further influenced by more systemic processes. We used a mouse model to show that mice exposed to ionizing radiation and subsequently transplanted with unirradiated donor tissue preferentially develop ER-negative breast cancers (23). These tumors exhibit a gene expression program characterized by signatures of inflammation and stem cell biology. Somewhat surprisingly, the murine host radiation profile also segregates sporadic human breast cancers according to intrinsic subtype, i.e. basal from luminal, and within basal cancers, the irradiated murine host profile mediated by TGF β associated with claudin-low cancers (24). This bioinformatic analysis suggests that common processes may underlie the etiology of both radiation-preceded and sporadic basal-type cancers. These data led to the hypothesis that host biology profoundly influences the etiology of breast cancer intrinsic subtypes (25).

As puberty is a period of significant physiological changes that alters the hormonal milieu that in turn directs mammary morphogenesis, in this study we used a mammary chimera model to compare the development of *Trp53* null cancer as a function of host age. More tumors arose from *Trp53* null outgrowths in adult mice compared to those transplanted during puberty, but the influence of puberty was manifested in development of rapidly growing, strongly ER-positive luminal tumors. We found that the transcriptional profile of the features that differ between tumors arising from juvenile versus adult transplantation segregates human luminal intrinsic breast cancer subtypes.

Methods

Animals

All animal experiments were performed at Lawrence Berkeley National Laboratory with institutional review and approval. BALB/c mice were purchased from the Jackson Laboratory (Bar Harbor, ME) and housed four per cage, fed with Lab Diet 5008 chow and water *ad libitum*. *Trp53* null BALB/c mice were bred in-house under similar conditions. For transplantation experiments, the epithelial rudiments in inguinal glands of 3-week-old mice were surgically removed. At 5 or 10 weeks of age, both cleared mammary glands of host mice were transplanted with a ~1 mm³ fragment of *Trp53* null BALB/c mammary gland harvested and pooled from 3 or more inguinal glands of 8- to 10-week-old donor mice. Mice were monitored by palpation 2–3 times per week for 13 months. Once a palpable tumor was detected, tumors were measured with calipers twice weekly until reaching 1cm³, at which point the first tumor was resected using survival surgery. Tumors were divided and frozen in liquid nitrogen for RNA extraction, or formalin-fixed followed by paraffin embedding. The

mouse was further observed until the ipsilateral recurrence or a second tumor developed in the contralateral fatpad, which was monitored as above. If no tumors developed by experiment termination, which was 13 months after transplantation, then a wholemount was prepared to confirm transplantation efficiency. A gross necropsy was performed upon termination. An informative transplant was defined as that which had an epithelial outgrowth evident by tumor development or in the wholemount at sacrifice.

Immunohistochemistry

Sections were deparaffinized and rehydrated prior to antigen unmasking according to manufacturer's instructions (Vector Labs, #H-3300), washed once with phosphate buffer saline and blocked with 0.5% casein and 0.1% Tween20/PBS for 1 hr at room temperature. Primary antibodies to ER (C1355) (Millipore/Upstate, #06-935), PR (Fisher Scientific, RM-9102-S0), Foxa1 (Abcam, ab23738), Gata3 (Santa cruz, SC-268), or phospho-IGF1 receptor (IGFR; Abcam, Ab39398) were diluted in Superblock Blocking Buffer (Pierce, #37515) and incubation was done at 4 degrees C, overnight. The slides were then washed, followed by incubation with peroxidase-conjugated secondary antibody, washed and counterstained with hematoxylin. Histopathological characteristics of the tumors were reviewed by two observers blinded to the experimental details of the mouse models. Estrogen receptor status was scored using the Allred method(26).

Expression Profiling

Total RNA quality and quantity was determined using Agilent 2100 Bioanalyzer and Nanodrop ND-1000. IlluminaMouse WG-6 v2.0 Expression Beadchips were used according to manufacturer's protocol. The raw values (non-normalized, non-background-corrected) were exported from Beadstudio and read into R/Bioconductor using the Lumi package. Intensity values were then log₂ transformed and quantile normalized. Background subtraction was not performed. The main effect of no background correction for Illumina data is that the fold-change estimation for low expression probes tends to be lower, but low expression yet high fold-change probes are more likely to be false positives. Gene expression data is archived on GEO under accession number GSE56726.

Unsupervised hierarchical clustering was done using Gene Cluster v3.0 software and heatmaps were visualized using Java TreeView v1.1.4r3 software. Expression data was mean centered. Gene clustering was done by an uncentered-correlation; array clustering was done by Spearman Rank correlation; complete linkage. Significance of Analysis of Microarray (SAM) analysis was done in a tandem-bootstrapping scheme as previously described (23). This approach derived a profile of 243 genes modulated by at least 1.5-fold in JH tumors, in 100% (13/13) of the secondary bootstraps. Enriched pathways within the 243 genes were identified with Ingenuity Pathway Analysis.

Statistical Analysis

Statistical analysis was performed using Prism (GraphPad). Time to 2×2mm³ tumor occurrence per informative fatpad was plotted using the Kaplan-Meier method with significance determined by the log-rank test. Tumor growth curves in a treatment group were fitted to an exponential curve and then averaged into one curve for each treatment

group, as previously reported (23). Differences between treatment groups was determined using the Chi-square test, Mann-Whitney test or two-tailed Student's t-test, which were considered statistically significant at $p < 0.05$. The K-S test was used to determine the difference in distributions of human breast cancers that were classified by the centroids and then stratified by plotting in two-dimensions.

Results

Age at transplantation affects *Trp53* null mammary carcinogenesis

The mouse mammary gland develops after birth, starting at 4 weeks of age with the onset of the ovarian hormones of puberty. The inguinal mammary gland can be divested of its endogenous epithelia at three weeks of age (27). Afterwards, a mammary fragment from a donor mouse can be transplanted into the empty fat pad and it will grow out to form a ductal tree after 6–8 weeks. Here, we employ the mammary chimera model to test the effect of age by characterizing the occurrence and type of tumors arising from *Trp53* null outgrowths initiated in a host undergoing puberty compared to those that arise from transplantation into an adult. *Trp53* null mammary fragments from 8- to 10-week-old syngeneic donors were transplanted into 5 week-old (juvenile) or 10 week-old (adult) BALB/c hosts; tumor occurrence was monitored for 13 months after transplantation (Figure 1A). Significantly more palpable tumors were obtained in mice that were adults at transplantation (Figure 1B). The extent of morphogenesis and successful transplantation frequency were comparable regardless of age at transplantation and the average size of neoplastic nodules (i.e. those that did not form frank, palpable tumors) evident in carmine-stained outgrowth wholemounts was similar for transplantation at each host age (data not shown). Age at transplantation did not affect the distribution of tumor histopathology (summarized in supplemental table 1), which included adenocarcinomas, spindle cell carcinomas, and squamous carcinomas as previously reported for this *Trp53* null model (23). AH tumors ($n=89$) had a median latency of 347 days, and 55% of informative fatpads were tumor-bearing by experiment termination. In contrast, the median latency of JH tumors ($n=55$) could not be calculated since only 27% of informative fatpads developed palpable tumors.

Transplantation during puberty results in more aggressive tumors

Although fewer tumors arose from transplantation during puberty, once the tumor was detected, JH tumors grew significantly faster compared to adult hosts (Figure 2A). The tumor growth rate of tumors arising from transplantation to adults was comparable to that observed in previous experiments (23). Moreover the difference of tumor growth rate was replicated in cohort of mice transplanted as adults versus juveniles in an independent study (28). Mitotic figures that included the spectrum of condensed chromosome states (Figure 2B) were quantified in high-powered fields of view ($n=10$) per hematoxylin and eosin (H&E)-stained tumor. Consistent with increased growth rate, mitotic figures increased two-fold in JH tumors compared to AH tumors (Figure 2C). We next examined the degree of vascular perfusion. Red blood cells are auto-fluorescent under the UV filter in H&E stained tissue. We quantified the average area of red blood cell cross-sections encapsulated within a membrane lining to exclude areas of hemorrhage to measure the size of perfused vessels (Figure 2D). The size of perfused vessels in JH tumors was twice that of AH tumors

(Figure 3E). Thus, the age of the host, juvenile or adult, at the time of *Trp53 null* mammary transplantation affects the features of tumors that arise a year later.

Transplantation during puberty results in a luminal breast cancer subtype

The BALB/c *Trp53 null* mammary transplant model recapitulates the histological (29,30) and molecular diversity of human breast cancer (24,31). 80% of the tumors arising from JH were ER+ by the Allred Score (26), compared to 70% ER+ AH tumors (Figure 3A), similar to that previously observed from transplantation in adult mice (23,28). Furthermore, comparing ER+ tumors between JH and AH tumors, those from JH tumors were much more highly ER+ (Figure 3C; JH, mean 11–33%, max >66%; AH, mean 1–10%, max 11–33%). We also examined other canonical luminal markers including progesterone receptor (PR) and *Foxa1*. 50% of JH tumors (8/16) were positive for PR, compared to less than 40% of AH tumors (4/11). Similarly, the PR immunoreactivity in PR+ tumors from JH tend to be higher (JH, mean 11–30%; AH, mean 2–10%). 80% of JH tumors (8/10) were also positive for *Foxa1* while around 70% AH tumors (7/11) were *Foxa1* positive. The intensity and frequency of *Foxa1* positivity were comparable between JH and AJ tumors. We also examined the *Gata3* level by immunostaining, however, the results were not informative, with only one positive nuclear staining out of 20 tumors (10 JH and 10 AH). Overall, JH tumors exhibit features of a luminal cancer subtype.

We next conducted genome-wide microarray analysis using total RNA from JH tumors (n=15) and AH (n=12) tumors using Illumina Mouse WG-6 V2.0 Beadchips. Unsupervised hierarchical clustering (UHC) of all tumors did not segregate JH from AH tumors (data not shown). Significance analysis of microarray (SAM) analysis was done in a tandem-bootstrapping scheme, as previously reported (23), to derive a profile of genes modulated by at least 1.5-fold in 100% (13/13) of the secondary bootstraps in JH tumors. This yielded 243 genes (Supplemental table 2) that represented the biology of JH tumors compared to AH tumors (Table S1). UHC of the 27 tumors by these 243 genes resulted in segregation of most JH tumors apart from AH tumors (data not shown). Ingenuity Pathway Analysis (IPA) revealed that the global processes occurring in these 243 genes included embryonic development, organ development, and organ morphology (Figure 4A, IPA score 43); and cellular growth & proliferation, cancer, and tumor morphology (Figure 4B, IPA score 38). Consistent with the high ER protein expression detected in these tumors, there was a clear luminal gene expression program induced by the JH: *Foxa1*, *Areg*, and *Krt18* (Figure 4C). Additionally, *Igf2* and *Ccnd1* (Cyclin D1) transcripts were also increased, consistent with the increased mitotic index detected in JH tumors (32,33). Beyond growth induction, the *Areg* gene product has been reported to have pro-angiogenic properties, which would be consistent with the increased perfusion observed in JH tumors (34).

Enhanced IGF1 signaling associates with the luminal subtype of breast cancer

Studies in human and mouse have shown that enhanced IGF signaling is associated with breast cancer phenotype (reviewed in (35)), including poor prognosis(36), and IGF signaling regulates proliferation in the normal mammary gland (37,38). Since JH tumors were highly proliferative and exhibited an increase in *Igf2* transcript, we examined phospho-IGF receptor (IGFR) levels in JH tumors. Both *Igf1* and *Igf2* bind to IGFR and ligand binding of the

IGFR leads to its phosphorylation. Phosphorylated IGFR was detected with an antibody targeting the Y1161 residue, which represents the activated state of the receptor. Positive cells were located near the tumor border were characterized by membrane staining (Figure 4D and E). Phosphorylated IGFR staining was semi-quantitatively assessed as the percent of a tumor that exhibited positive staining. Phosphorylated IGFR was increased 25-fold in JH tumors ($p=0.026$) compared to AH tumors (Figure 4F).

Human orthologs of the JvA243 profile segregates luminal breast cancers

The high ER protein expression and luminal transcriptional program in the JH tumors clearly suggested that these tumors were of a luminal subtype. We then determined the utility of 243-gene JH profile in discerning differences between human breast cancers using the Fredlund data set, which represents 1608 breast cancers compiled from 10 independent data sets on the Affymetrix U133A platform. Human orthologs of 161 genes, represented by 314 probes, of the 243 mouse genes were present on the Affymetrix Human U133A platform. To further explore this association, we developed a JvA centroid table, which maintains the relative direction of the genes that are differentially expressed in tumors arising in juvenile versus adult hosts (Supplemental table 3). Genes in the JvA centroid table were the human homologs mouse JvA genes, which are referred to as the JHh and AHh centroids, respectively. Human breast cancers ($n=1608$) from Fredlund were classified and the correlation values of each sample to each of the two centroids were plotted as x and y coordinates. This classification revealed stratification of human breast luminal versus basal tumors. Luminal human breast cancers shifted away from the positive axis representing adult host tumors, while basal-like cancers shifted towards this axis (Figure 5A, $p=1.11E-33$). Interestingly, when only luminal A and B tumors were compared, the distribution of human luminal A (39) tumors suggested that they were more similar to murine tumors arising from tissue transplanted during puberty, while the distribution of luminal B (LumB) tumors was shifted towards the axis representing adult host tumors (Figure 5B & C, $p=3.17E-16$).

To further explore this association, we then applied the JvA human orthologs gene list to the data set from (40) (GSE4922), which contains 137 LumA or LumB human breast cancers. JvA human orthologs segregated LumA and LumB tumors. LumB cancers comprised 30% of sub-tree 1 versus 63% of sub-tree 2 (chi-square, $p<0.0003$) (Figure 6A). Since it is known that LumB cancers are much more proliferative than LumA cancers (reviewed in (8)), we determined how the proliferation program in the 243 genes affected segregation. Removal of 31 proliferation-related genes in the 161 human orthologs left 130 human genes represented by 240 probes (Table S2). The proliferation-divested profile showed even stronger segregation of LumB cancer in the Ivshina data set (16% in sub-tree 1, 63% in sub-tree 2; chi-square, $p<0.0001$) (Figure 6B). The same effect was observed on 110 Grade-1 LumA or LumB cancers in (41) in that LumB tumors comprised 10% of sub-tree 1, but 39% of sub-tree 2 (chi-square, $p<0.001$) (Figure 6C). Effective segregation of LumA from LumB cancers without the proliferation-related genes suggests that the JvA 243 profile captures a biological distinction between LumA and LumB that is more than just increased proliferation. Taken together, the bioinformatic analyses suggest that the JvA gene list associates with a distinct luminal breast cancer subtype.

Discussion

To date, studies using the *Trp53* null mammary chimera at different ages, genotypes or physiological states suggest that it is a robust model for studying breast cancer diversity (23,31,42–44). Our studies using this model suggest that the host environment profoundly influences the type of tumor that eventually develops, long after mammary outgrowth is complete. Here we show that the age at transplantation elicits phenotypically and genomically distinct tumors that have features strongly reminiscent of the human luminal intrinsic subtypes. Although transplantation of adult hosts generated more tumors compared to those transplanted during puberty, tumors arising from juvenile host grew faster, had more mitoses and were better perfused than those arising from outgrowths initiated in adult mice. Moreover, ER and phosphorylated IGFR staining were significantly enhanced in JH tumors. This phenotype was evident in the distinct genomic profile JvA, defined by comparison of tumors arising in JH versus AH hosts. JH tumors were characterized by elevated *Igf2*, *Fgfr2*, and *FoxA1*. Notably, the JvA was informative in regards to intrinsic tumor types in human breast cancer. Centroids defined by the human orthologs of the JvA profile stratified luminal from basal-like human breast cancers and luminal A from luminal B breast cancers. In support of this, JvA clustered luminal A and B intrinsic subtypes across public data sets.

An intriguing question is how the physiology and microenvironment during puberty promotes the development of highly ER+ mammary cancers. The mammary gland in mice and humans develops into maturity after birth. The onset of puberty initiates the estrus cycle that releases cyclical surges of estrogen and progesterone, two of the main hormones that induce ductal morphogenesis. Concomitantly, growth hormone and IGF stimulate longitudinal growth of the entire organism, while also being essential regulators of mammary gland development (37,38). Phosphorylated IGFR staining was strikingly elevated in the highly ER positive JH tumors compared to AH tumors. Involvement of IGF signaling is consistent with the highly ER-positive luminal phenotype. It has been shown that in mice, serum IGF-1 level was significantly higher during the late puberty (5–8 weeks of age) compared to the level during the early puberty (3–5 weeks of age) (45). It is possible that this growth factor surge promotes the carcinogenesis of JH tumor while for AH tumor, such growth-stimulation is lacking. This potential mechanism will be investigated in the further studies where different hormones are evaluated at different ages. Notably proliferation mediated by IGF-1 is important in cancer overall, is strongly associated with poor prognosis in breast tumors (36) and increases susceptibility in familial breast cancer (46).

Given the diversity of *Trp53* tumor phenotypes, these specimens provide a meaningful model to further examine specific genomic alterations associated with particular tumor types. One means by which host physiology may influence tumor type is by causing epigenetic changes. The Cancer Genome Atlas project integrated copy number, RNA, methylation status and miRNA data from approximately 300–460 human breast cancer genomes for each breast cancer subtype (9). Breast cancers positive for ER have a distinct methylome profile compared to the more aggressive ER-negative cancers (47). Methylation is a key component of differentiation-associated patterns of transcription in normal

development of the mammary gland (48). Both hypo- and hyper-methylation changes are associated with disease. DNA methylation can confer long term memory of early life events (49). Consistent with this, high estrogen exposure during neonatal development induces epigenetic imprinting in the form of gene methylation that is reflected in uterine and prostate cancers arising later on in adulthood (50,51). Indeed breast cancer molecular subtypes defined by transcriptomic profiling can also be characterized by methylome profiling (52), suggesting that the two may go hand-in-hand. Identical hypermethylated genes occur in histologically normal ducts that are adjacent to pre-invasive and invasive lesions, suggesting a common loco-regional etiology mediated by methylation (9,53,54).

We speculate that the distinct tumor subtypes that arise as a function of host biology in the mammary chimera model could be rooted in factors that influence cell intrinsic processes of either initiation or early progression during specific physiological states, which in this case is puberty. The relative short age window of 5 weeks between transplantation resulting in JH and AH tumors suggest that events occurring in roughly the first month of transplant outgrowth impacts the specific tumor type. The transplanted tissue fragments contain about 2,000 epithelial cells that contain 1–4 stem cells based on functional repopulation assays (28). *Trp53* null tissue gives rise to morphologically normal ductal outgrowths by 3 months post-transplantation; over the course of the next 6–9 months morphologically aberrant lesions become evident. This effect of transplantation at different ages is consistent with our studies in irradiated hosts in which tumor type was affected even though only the host was irradiated months before tumor development. A strong radiation signature in the mammary gland expression profiles is present at 1 week after exposure, is much less robust at 4 weeks, and is no longer discernable 12 weeks after irradiation, yet is evident in tumors arising months later (23,28).

In multi-stage carcinogenesis models, cancer is initiated by genomically aberrant cells whose proliferation results in acquisition of additional mutations to establish the malignant phenotype. Concomitant subversion of tissue suppressive function, evasion of the immune system and recruitment of a permissive stroma involves a dynamic interplay between malignant and non-malignant cells that is equally important (25). Our data from the *Trp53* mammary chimera model shows that tumor latency and type is highly influenced by differences in host biology at the time of transplantation due to exogenous conditions (e.g. ionizing radiation exposure, diet) or endogenous factors (e.g. host genotype, age). The idea that tumor type is determined by biology outside the epithelial cell genome is provocative in that it suggests that tumor type is not the sum of random genomic alterations and that, once understood, such host biology might be a target for chemoprevention. Extrinsic carcinogenesis processes can be viewed in terms of environmental imprinting or ecological selection, although it is unclear which is more likely without more detailed studies or modeling. The mammary chimera model provides the means to somewhat uncouple cellular (i.e. initiation) and systemic responses to physiological or environmental (e.g. life style) factors during carcinogenesis.

Conclusions

Age is clearly a primary factor associated with the risk of detecting clinically evident cancer, but it has been less clear how age intersects with the carcinogenic process. Here, mammary *Trp53* null carcinogenesis advanced more rapidly from transplantation to adult hosts compared to pubertal hosts, but tumors arising from transplantation during puberty had more distinct hallmarks (e.g. faster growth rate, more mitoses, and greater perfusion) than those tumors arising from transplantation to an adult mouse. Preliminary data from middle-aged mice (i.e. transplanted at 10 months of age) indicate that tumorigenesis is reduced but the frequency of ER-negative tumors substantially increased (unpublished data). The mammary chimera model provides novel evidence that both the latency and subtype of cancer is strongly influenced by factors beyond genomic alterations within the tumor cells.

The distinct biology of murine tumors arising from tissue undergoing morphogenesis in the context of puberty suggests that neoplastic transformation at a young age promotes a luminal tumor phenotype. These data support the notion that tumor intrinsic subtype is influenced by physiological status at the time of putative initiation. Future studies will determine how systemic factors particular to puberty act to promote luminal-type tumors. Potential mechanisms include those affecting initiation, supporting survival of cells with particular mutations, or generating a stroma permissive for particular initiation events.

Supplementary Material

Refer to Web version on PubMed Central for supplementary material.

Acknowledgments

The authors would like to thank Dr. Sylvain Costes (Lawrence Berkeley National Lab) for assistance with statistics and the GeneSys Research Institute (Tufts University School of Medicine) for expression profiling. This research was supported by a pre-doctoral fellowship to DHHN from the DOD-BCRP, funding from the Department of Energy, Office of Biological and Environmental Research program on Low Dose Radiation (JHM, MHBH) and the National Cancer Institute of the National Institutes of Health under Award Number U54CA149233 (LH, MHBH).

Abbreviations

ER	estrogen receptor
SAM	significance of analysis of microarray
IGF	insulin-like growth factor
IGFR	insulin-like growth factor receptor
JH	juvenile hosts
AH	adult hosts
H&E	hematoxylin & eosin
UHC	Unsupervised hierarchical clustering
IPA	Ingenuity Pathway Analysis

LumA	luminal A breast cancer
LumB	luminal B breast cancer

References

1. Gusterson BA, Gelber RD, Goldhirsch A, Price KN, Save-Soderborgh J, Anbazhagan R, et al. Prognostic importance of c-erbB-2 expression in breast cancer. International (Ludwig) Breast Cancer Study Group [see comments]. *J Clin Oncol.* 1992; 10(7):1049–1056. [PubMed: 1351538]
2. Rakha EA, El-Sayed ME, Green AR, Lee AH, Robertson JF, Ellis IO. Prognostic markers in triple-negative breast cancer. *Cancer.* 2007; 109(1):25–32. [PubMed: 17146782]
3. Rakha EA, Elsheikh SE, Aleskandarany MA, Habashi HO, Green AR, Powe DG, et al. Triple-negative breast cancer: distinguishing between basal and nonbasal subtypes. *Clin Cancer Res.* 2009; 15(7):2302–2310. [PubMed: 19318481]
4. Perou CM, Børresen-Dale A-L. *Systems Biology and Genomics of Breast Cancer.* Cold Spring Harbor Perspectives in Biology. 2011; 3(2)
5. Perou CM, Sorlie T, Eisen MB, van de Rijn M, Jeffrey SS, Rees CA, et al. Molecular portraits of human breast tumours. *Nature.* 2000; 406(6797):747–752. [PubMed: 10963602]
6. Sorlie T, Perou CM, Tibshirani R, Aas T, Geisler S, Johnsen H, et al. Gene expression patterns of breast carcinomas distinguish tumor subclasses with clinical implications. *Proc Natl Acad Sci U S A.* 2001; 98(19):10869–10874. [PubMed: 11553815]
7. Prat A, Parker JS, Karginova O, Fan C, Livasy C, Herschkowitz JI, et al. Phenotypic and molecular characterization of the claudin-low intrinsic subtype of breast cancer. *Breast Cancer Res.* 2010; 12(5):R68. [PubMed: 20813035]
8. Creighton CJ. The molecular profile of luminal B breast cancer. *Biologics.* 2012; 6:289–297. [PubMed: 22956860]
9. Network CGA. Comprehensive molecular portraits of human breast tumours. *Nature.* 2012; 490(7418):61–70. [PubMed: 23000897]
10. Visvader JE. Cells of origin in cancer. *Nature.* 2011; 469(7330):314–322. [PubMed: 21248838]
11. Liu X, Holstege H, van der Gulden H, Treur-Mulder M, Zevenhoven J, Velds A, et al. Somatic loss of BRCA1 and p53 in mice induces mammary tumors with features of human BRCA1-mutated basal-like breast cancer. *Proc Natl Acad Sci U S A.* 2007; 104(29):12111–12116. [PubMed: 17626182]
12. Molyneux G, Geyer FC, Magnay FA, McCarthy A, Kendrick H, Natrajan R, et al. BRCA1 basal-like breast cancers originate from luminal epithelial progenitors and not from basal stem cells. *Cell Stem Cell.* 2010; 7(3):403–417. [PubMed: 20804975]
13. Proia TA, Keller PJ, Gupta PB, Klebba I, Jones AD, Sedic M, et al. Genetic Predisposition Directs Breast Cancer Phenotype by Dictating Progenitor Cell Fate. *Cell stem cell.* 2011; 8(2):149–163. [PubMed: 21295272]
14. Jacquemier J, Charafe-Jauffret E, Monville F, Esterni B, Extra JM, Houvenaeghel G, et al. Association of GATA3, P53, Ki67 status and vascular peritumoral invasion are strongly prognostic in luminal breast cancer. *Breast Cancer Res.* 2009; 11(2):R23. [PubMed: 19405945]
15. Kouros-Mehr H, Bechis SK, Slorach EM, Littlepage LE, Egeblad M, Ewald AJ, et al. GATA-3 Links Tumor Differentiation and Dissemination in a Luminal Breast Cancer Model. *Cancer Cell.* 2008; 13(2):141–152. [PubMed: 18242514]
16. Voduc D, Cheang M, Nielsen T. GATA-3 Expression in Breast Cancer Has a Strong Association with Estrogen Receptor but Lacks Independent Prognostic Value. *Cancer Epidemiology Biomarkers & Prevention.* 2008; 17(2):365–373.
17. Castiglioni F, Terenziani M, Carcangiu ML, Miliano R, Aiello P, Bertola L, et al. Radiation effects on development of HER2-positive breast carcinomas. *Clin Cancer Res.* 2007; 13(1):46–51. [PubMed: 17200337]

18. Broeks A, Braaf LM, Wessels LF, van de Vijver M, De Bruin ML, Stovall M, et al. Radiation-associated breast tumors display a distinct gene expression profile. *Int J Radiat Oncol Biol Phys*. 2010; 76(2):540–547. [PubMed: 20117289]
19. Yang XR, Chang-Claude J, Goode EL, Couch FJ, Nevanlinna H, Milne RL, et al. Associations of Breast Cancer Risk Factors With Tumor Subtypes: A Pooled Analysis From the Breast Cancer Association Consortium Studies. *Journal of the National Cancer Institute*. 2011; 103(3):250–263. [PubMed: 21191117]
20. Roman-Perez E, Casbas-Hernandez P, Pirone J, Rein J, Carey L, Lubet R, et al. Gene expression in extratumoral microenvironment predicts clinical outcome in breast cancer patients. *Breast Cancer Research*. 2012; 14(2):R51. [PubMed: 22429463]
21. Finak G, Bertos N, Pepin F, Sadekova S, Souleimanova M, Zhao H, et al. Stromal gene expression predicts clinical outcome in breast cancer. *Nat Med*. 2008; 14:518–527. [PubMed: 18438415]
22. Lee S, Stewart S, Nagtegaal I, Luo J, Wu Y, Colditz G, et al. Differentially Expressed Genes Regulating the Progression of Ductal Carcinoma in Situ to Invasive Breast Cancer. *Cancer Research*. 2012
23. Nguyen DH, Oketch-Rabah HA, Illa-Bochaca I, Geyer FC, Reis-Filho JS, Mao JH, et al. Radiation Acts on the Microenvironment to Affect Breast Carcinogenesis by Distinct Mechanisms that Decrease Cancer Latency and Affect Tumor Type. *Cancer Cell*. 2011; 19(5):640–651. [PubMed: 21575864]
24. Nguyen DH, Fredlund E, Zhao W, Perou CM, Balmain A, Mao J-H, et al. Murine Microenvironment Metaprofiles Associate with Human Cancer Etiology and Intrinsic Subtypes. *Clin Cancer Research*. 2013; 19(6):1353–1362.
25. Barcellos-Hoff MH. Does Microenvironment Contribute to the Etiology of Estrogen Receptor Negative Breast Cancer? *Clin Cancer Res*. 2013; 19(3):541–548. [PubMed: 23325583]
26. Harvey JM, Clark GM, Osborne CK, Allred DC. Estrogen receptor status by immunohistochemistry is superior to the ligand-binding assay for predicting response to adjuvant endocrine therapy in breast cancer. *J Clin Oncol*. 1999; 17(5):1474–1481. [PubMed: 10334533]
27. DeOme KB, Faulkin LJ Jr, Bern HA, Blair PB. Development of mammary tumors from hyperplastic alveolar nodules transplanted into gland-free mammary fat pads of female C3H mice. *Cancer Res*. 1959; 19(5):515–520. [PubMed: 13663040]
28. Tang J, Fernandez-Garcia I, Vijayakumar S, Martinez-Ruiz H, Illa-Bochaca I, Nguyen DH, et al. Irradiation of juvenile, but not adult, mammary gland increases stem cell self-renewal and estrogen receptor negative tumors. *Stem Cells*. 2013; 32(3):649–661. [PubMed: 24038768]
29. Jerry DJ, Kittrell FS, Kuperwasser C, Laucirica R, Dickinson ES, Bonilla PJ, et al. A mammary-specific model demonstrates the role of the p53 tumor suppressor gene in tumor development. *Oncogene*. 2000; 19(8):1052–1058. [PubMed: 10713689]
30. Rajkumar L, Kittrell F, Guzman R, Brown P, Nandi S, Medina D. Hormone-induced protection of mammary tumorigenesis in genetically engineered mouse models. *Breast Cancer Research*. 2007; 9(1):R12. [PubMed: 17257424]
31. Herschkowitz JI, Zhao W, Zhang M, Usary J, Murrow G, Edwards D, et al. Comparative oncogenomics identifies breast tumors enriched in functional tumor-initiating cells. *Proceedings of the National Academy of Sciences*. 2011; 109(8):2778–2783.
32. Wang TC, Cardiff RD, Zukerberg L, Lees E, Arnold A, Schmidt EV. Mammary hyperplasia and carcinoma in MMTV-cyclin D1 transgenic mice. *Nature*. 1994; 369:669–671. [PubMed: 8208295]
33. Klos KS, Kim S, Alexander CM. Genotoxic exposure during juvenile growth of mammary gland depletes stem cell activity and inhibits Wnt signaling. *PLoS One*. 2012; 7(11):e49902. [PubMed: 23185480]
34. Ma L, Gauvill e C, Berthois Y, Millot G, Johnson GR, Calvo F. Antisense expression for amphiregulin suppresses tumorigenicity of a transformed human breast epithelial cell line. *Oncogene*. 1999; 18(47):6513–6520. [PubMed: 10597254]
35. Kleinberg DL, Wood TL, Furth PA, Lee AV. Growth hormone and insulin-like growth factor-I in the transition from normal mammary development to preneoplastic mammary lesions. *Endocrine Reviews*. 2009; 30(1):51–74. [PubMed: 19075184]

36. Creighton CJ, Casa A, Lazard Z, Huang S, Tsimelzon A, Hilsenbeck SG, et al. Insulin-Like Growth Factor-I Activates Gene Transcription Programs Strongly Associated With Poor Breast Cancer Prognosis. *Journal of Clinical Oncology*. 2008; 26(25):4078–4085. [PubMed: 18757322]
37. Ruan W, Kleinberg DL. Insulin-Like Growth Factor I Is Essential for Terminal End Bud Formation and Ductal Morphogenesis during Mammary Development. *Endocrinology*. 1999; 140(11):5075–5081. [PubMed: 10537134]
38. Ruan W, Fahlbusch F, Clemmons DR, Monaco ME, Walden PD, Silva AP, et al. SOM230 Inhibits Insulin-Like Growth Factor-I Action in Mammary Gland Development by Pituitary Independent Mechanism: Mediated through Somatostatin Subtype Receptor 3? *Molecular Endocrinology*. 2006; 20(2):426–436. [PubMed: 16223973]
39. Kolumam GA, Thomas S, Thompson LJ, Sprent J, Murali-Krishna K. Type I interferons act directly on CD8 T cells to allow clonal expansion and memory formation in response to viral infection. *J Exp Med*. 2005; 202:637–650. [PubMed: 16129706]
40. Hilton HN, Graham JD, Kantimm S, Santucci N, Cloosterman D, Huschtscha LI, et al. Progesterone and estrogen receptors segregate into different cell subpopulations in the normal human breast. *Molecular and Cellular Endocrinology*. 2012; 361(1–2):191–201. [PubMed: 22580007]
41. Fredlund E, Staaf J, Rantala J, Kallioniemi O, Borg A, Ringner M. The gene expression landscape of breast cancer is shaped by tumor protein p53 status and epithelial-mesenchymal transition. *Breast Cancer Research*. 2012; 14(4):R113. [PubMed: 22839103]
42. Yan H, Blackburn AC, McLary SC, Tao L, Roberts AL, Xavier EA, et al. Pathways contributing to development of spontaneous mammary tumors in BALB/c-*Trp53*^{+/-} mice. *Am J Pathol*. 2010; 176(3)
43. Abba MC, Hu Y, Levy CC, Gaddis S, Kittrell FS, Hill J, et al. Identification of modulated genes by three classes of chemopreventive agents at preneoplastic stages in a p53-null mouse mammary tumor model. *Cancer Prev Res*. 2009; 2(2):175–184.
44. Zhang M, Behbod F, Atkinson RL, Landis MD, Kittrell F, Edwards D, et al. Identification of tumor-initiating cells in a p53-null mouse model of breast cancer. *Cancer Res*. 2008; 68(12):4674–4682. [PubMed: 18559513]
45. Callewaert F, Venken K, Kopchick JJ, Torcasio A, van Lenthe GH, Boonen S, et al. Sexual dimorphism in cortical bone size and strength but not density is determined by independent and time-specific actions of sex steroids and IGF-1: evidence from pubertal mouse models. *Journal of bone and mineral research : the official journal of the American Society for Bone and Mineral Research*. 2010; 25(3):617–626.
46. Werner H, Bruchim I. IGF-1 and BRCA1 signalling pathways in familial cancer. *The Lancet Oncology*. 2012; 13(12):e537–e544. [PubMed: 23182194]
47. Brent RL. Carcinogenic risks of prenatal ionizing radiation. *Seminars in Fetal and Neonatal Medicine*. 2013; (0)
48. Liu S-C, Alomran R, Chernikova SB, Lartey F, Stafford J, Jang T, et al. Blockade of SDF-1 after irradiation inhibits tumor recurrences of autochthonous brain tumors in rats. *Neuro-Oncology*. 2014; 16(1):21–28. [PubMed: 24335554]
49. Arnold JN, Magiera L, Kraman M, Fearon DT. Tumoral Immune Suppression by Macrophages Expressing Fibroblast Activation Protein-Alpha and Heme Oxygenase-1. *Cancer Immunology Research*. 2013
50. Li Y, Welm B, Podsypanina K, Huang S, Chamorro M, Zhang X, et al. Evidence that transgenes encoding components of the Wnt signaling pathway preferentially induce mammary cancers from progenitor cells. *Proc Natl Acad Sci USA*. 2003; 100:15853–15858. [PubMed: 14668450]
51. Gao C, Kozłowska A, Nechaev S, Li H, Zhang Q, Hossain DMS, et al. TLR9 Signaling in the Tumor Microenvironment Initiates Cancer Recurrence after Radiotherapy. *Cancer Research*. 2013; 73(24):7211–7221. [PubMed: 24154870]
52. Klug F, Prakash H, Huber Peter E, Seibel T, Bender N, Halama N, et al. Low-Dose Irradiation Programs Macrophage Differentiation to an iNOS⁺/M1 Phenotype that Orchestrates Effective T Cell Immunotherapy. *Cancer Cell*. 2013; 24(5):589–602. [PubMed: 24209604]

53. Rajaram M, Li J, Egeblad M, Powers RS. System-Wide Analysis Reveals a Complex Network of Tumor-Fibroblast Interactions Involved in Tumorigenicity. *PLoS Genet.* 2013; 9(9):e1003789. [PubMed: 24068959]
54. Sofia Vala I, Martins LR, Imaizumi N, Nunes RJ, Rino J, Kuonen F, et al. Low Doses of Ionizing Radiation Promote Tumor Growth and Metastasis by Enhancing Angiogenesis. *PLoS ONE.* 2010; 5(6):e11222. [PubMed: 20574535]

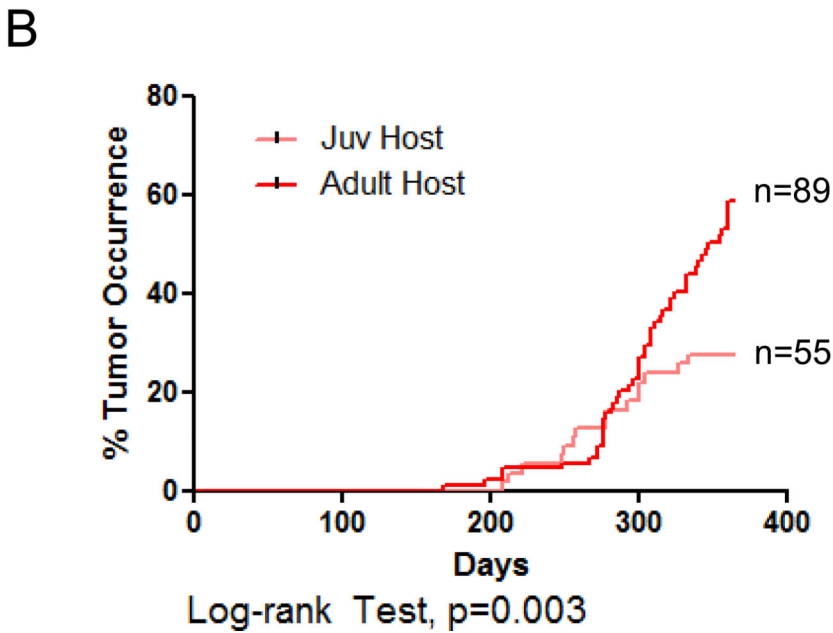
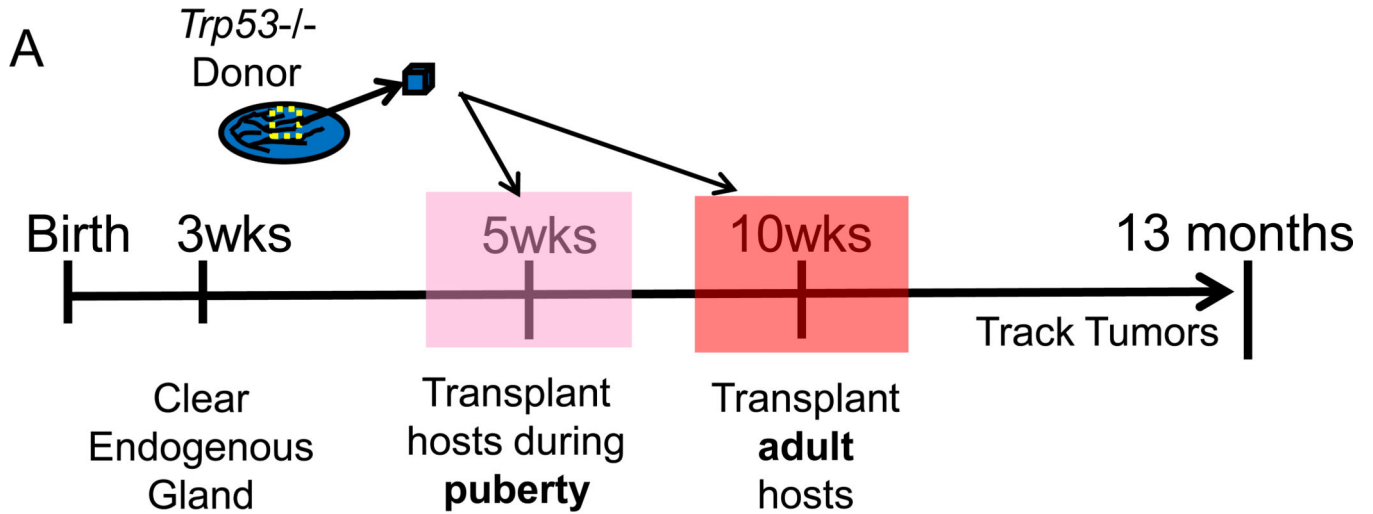


Figure 1. *Trp53* null transplantation into juvenile hosts delays tumorigenesis compared to adult hosts

(A) Cartoon of experimental scheme in which the epithelial rudiments of host mice were surgically removed from the inguinal mammary gland. A mammary fragment from a syngeneic *Trp53* null BALB/c mouse was transplanted into the empty fatpad at either 5 weeks of age (middle of puberty) or 10 weeks of age (young adult). Tumor development was tracked for 13 months. (B) Kaplan-Meier analysis tracking the time to tumor. Transplants into adult hosts (red) had a median tumor latency of 347 days, with 55% (n=89) of successful outgrowths forming tumors. Transplants into juvenile host fatpads (pink; n=55) formed tumors at a frequency of 27% after 13 months (Log-rank test, p=0.003).

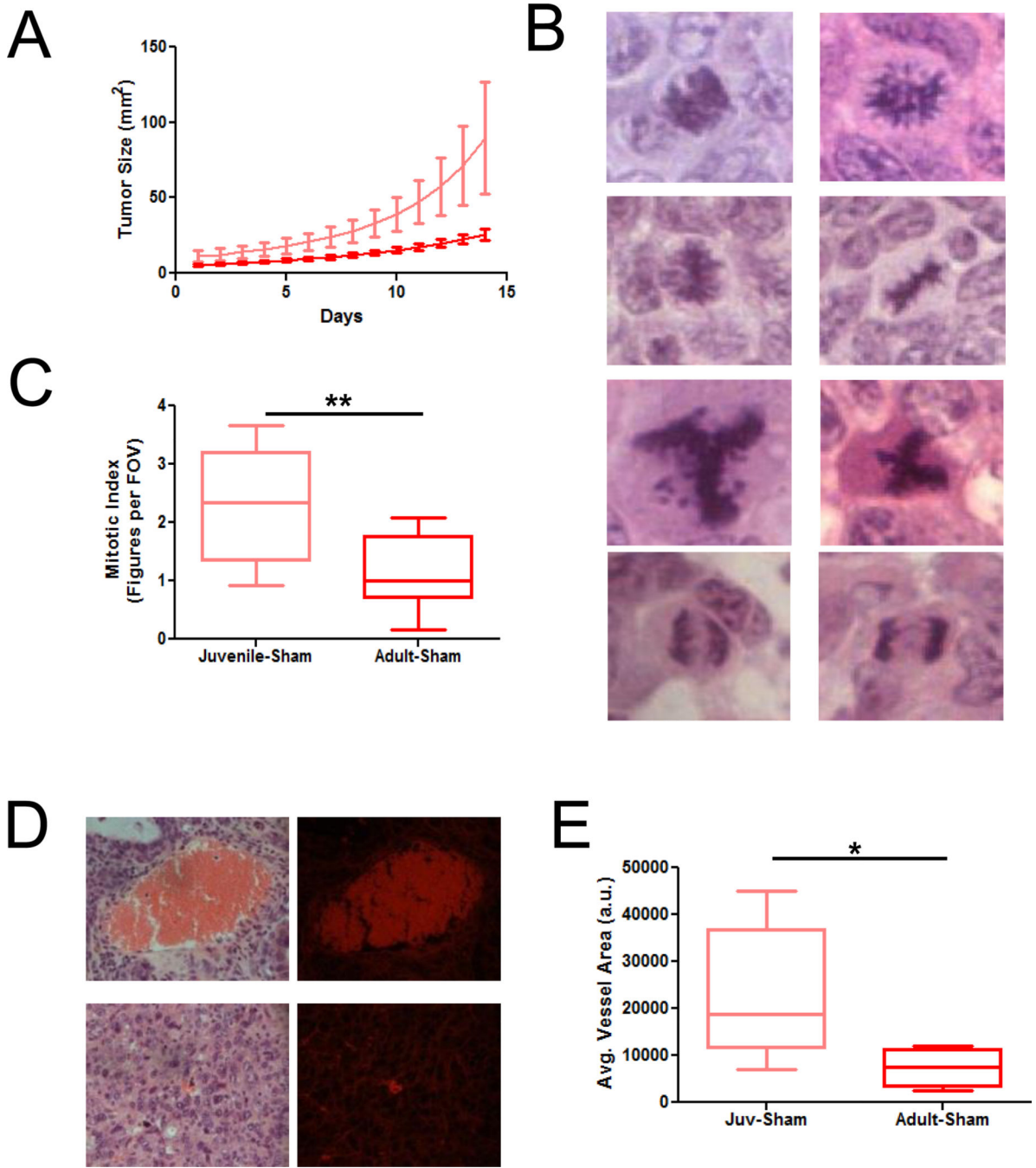


Figure 2. Tumors from transplantation during puberty grow faster than those arising from transplantation in adult hosts

(A) Tumors from transplants into 5 week-old juvenile hosts grew faster than those from 10-week-old (adult) hosts. (B) Mitotic index was calculated by counting mitotic figures representing the full range of condensed chromosomal states visualized by H&E staining. (C) Tumors from juvenile hosts (n=12) exhibited a 2-fold higher mitotic index than those from adult hosts (n=8) (**, p=0.009, Mann Whitney test). (D) The degree of tumor perfusion was quantified by measuring the average area of red blood cell clusters that were encapsulated in a membrane. Red blood cell clusters in tumor sections stained by H&E are

auto-fluorescent under UV. (E) Tumors arising from transplants into juvenile hosts (n=12) had 2-fold larger perfused blood vessels than those from adult hosts (n=8) (*, p=0.014, Mann Whitney test).

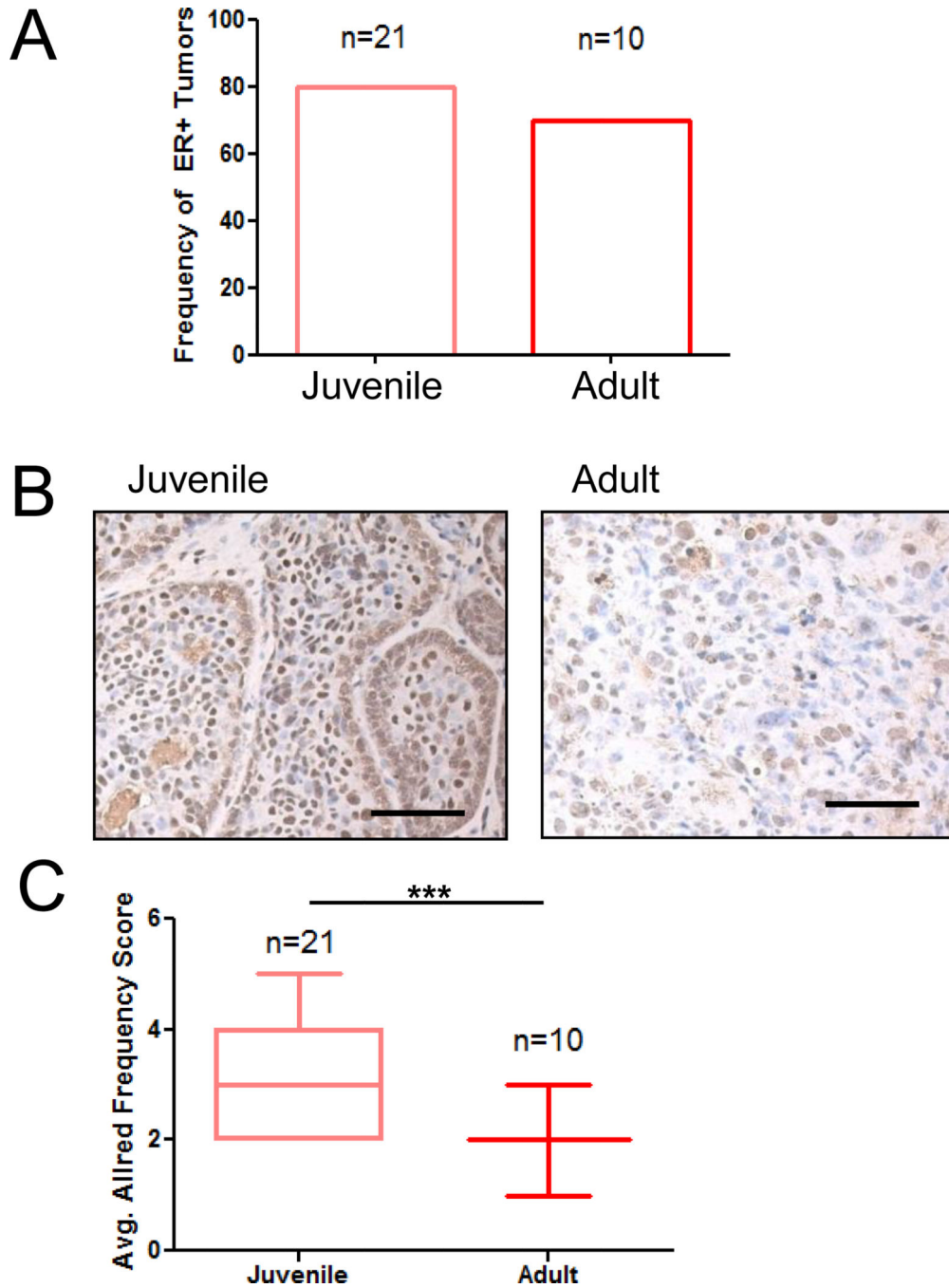


Figure 3. Tumors from transplantation during puberty are more highly immunoreactive for ER (A) 80% of tumors (n=21) from transplants into juvenile hosts were ER-immunoreactive compared to 70% of tumors (n=10) from transplants into adult hosts as classified according to the Allred score. (B) Representative images of ER immunohistochemistry in tumors from juvenile or adult hosts (bar, 60µm). (C) Comparison of the frequency component of the Allred score revealed that tumors from juvenile hosts were more immunoreactive for ER than tumors from adult hosts (juvenile, mean 11–33%, max >66%; adult, mean 1–10%, max 11–33%) (***, p=0.0004, Mann Whitney test).

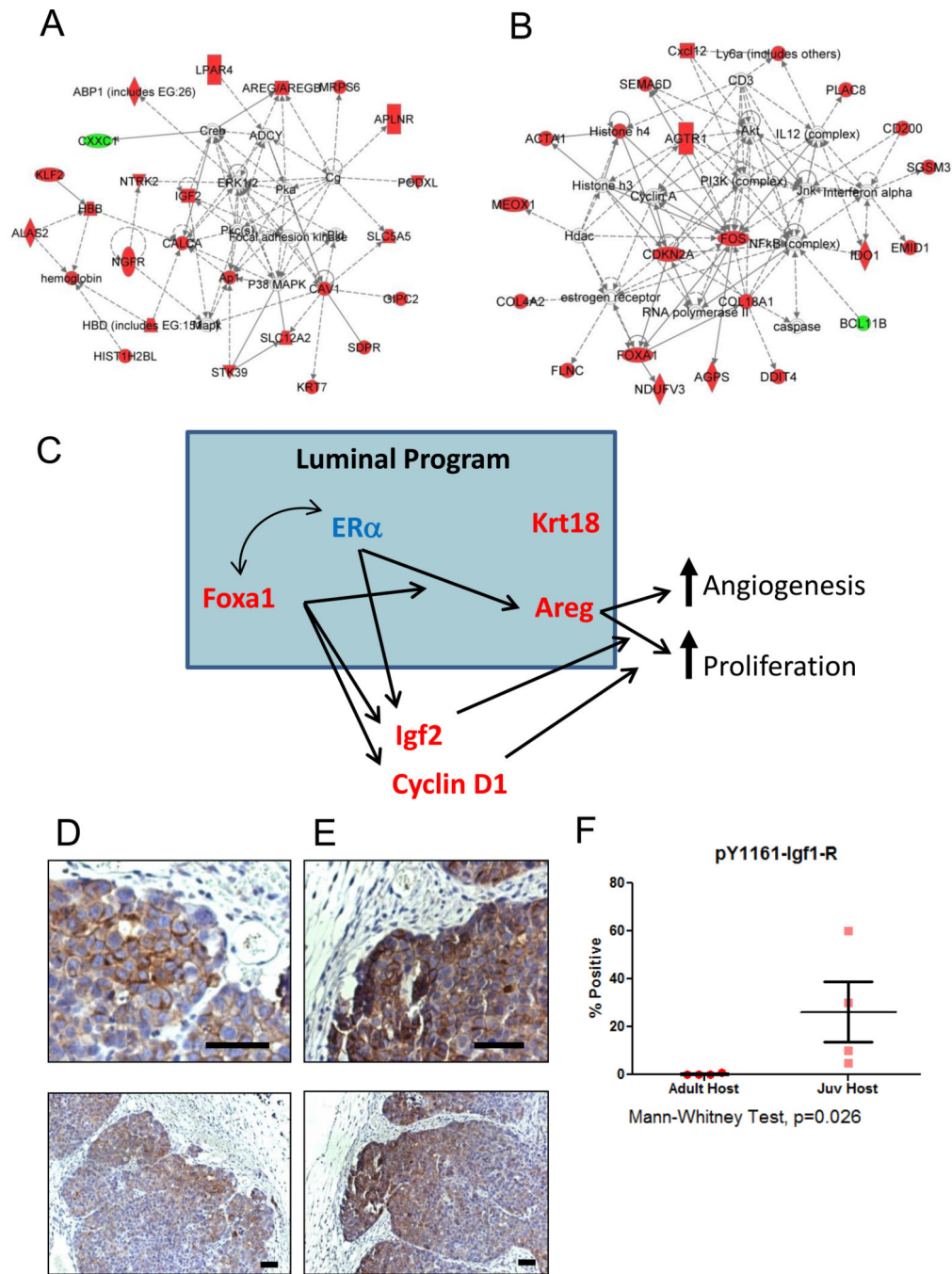


Figure 4. Gene expression analysis revealed a luminal transcriptional program in tumors arising from juvenile hosts

Genome-wide microarray analysis was done on tumors from juvenile hosts (n=15) or adult hosts (n=12). SAM-tandem-bootstrapping was done to identify 243 genes that were modulated by at least 1.5-fold in tumors from pubertal hosts compared to adult hosts. Ingenuity Pathway Analysis revealed two main biological processes with the 243-gene profile: embryonic development, organ development and organ morphology (A, IPA score 43); and cellular growth and proliferation, cancer, and tumor morphology (B, IPA score 38). (C) The 243 JvA gene profile represented canonical mammary luminal genes, including

Foxa1, *Krt18*, and *Areg*. Tumors arising from transplants in juvenile hosts or adult hosts were immunostained with the pY1161-IGFR antibody. (D) Cell membranes were weakly positive for pY1161-IGFR near the edge of AH tumors (Bar, 60 μ m). (E) Cell membranes were strongly positive for pY1161-IGFR near the edge of JH tumors (Bar, 60 μ m). (F) pY1161-IGFR staining was semi-quantitatively assessed as the percent of a tumor that exhibited positive staining. JH tumors exhibited a 25-fold increase in cells positive for phosphorylated-IGFR (Mann-Whitney test, $p=0.026$).

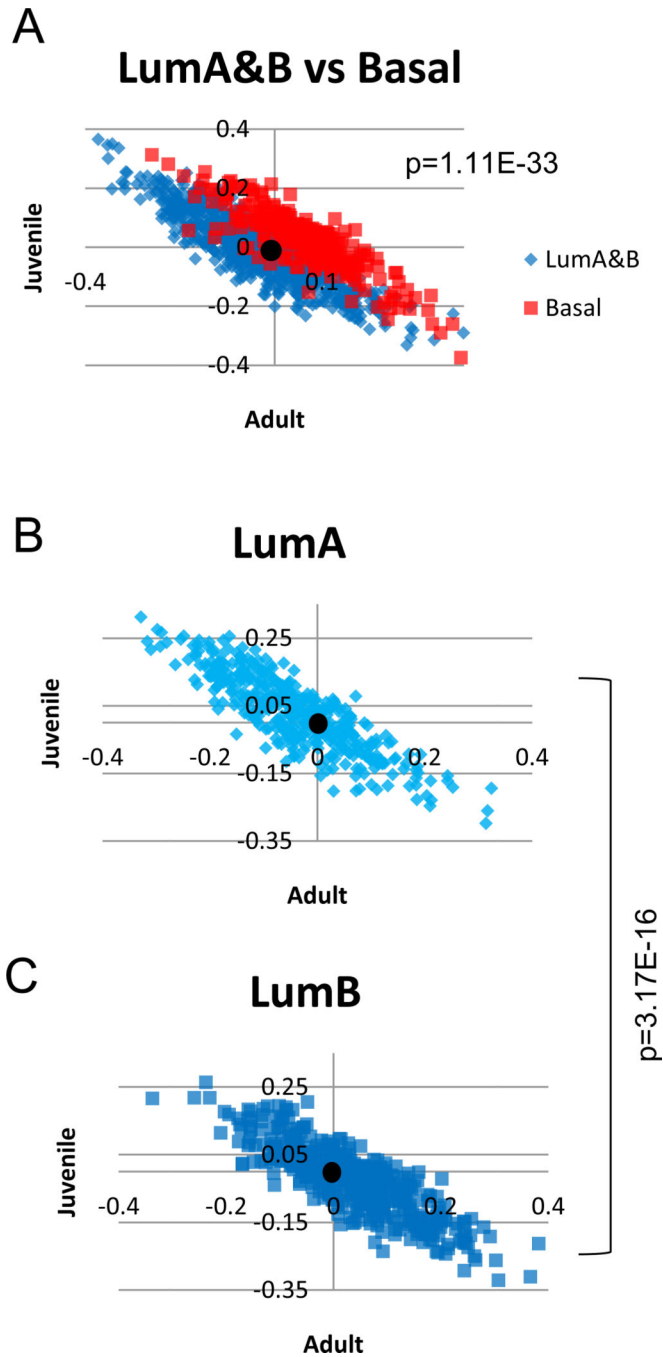


Figure 5. Luminal A human breast cancers are more similar to JH tumors
 (A) Centroids (JHh and AHh) representing the human orthologs of the JvA 243 gene profile were used to stratify 1,063 luminal (blue) or basal-like (red) human breast cancers (x-axis, adult host; y-axis, juvenile host). JHh vs AHh centroid stratification distinguished luminal cancers from basal-like cancers, with the distribution of basal-like cancers shifting towards the positive AHh axis (K-S test, $p=1.11E-33$). This suggests that basal-like cancers are more similar to tumors arising from transplantation to adult hosts. (B&C) The centroid stratification of luminal A and luminal B cancers shows that luminal A cancers shift towards

the positive JHh axis and away from the positive AHh axis, while luminal B are shifted towards the positive AHh axis and away from the positive JHh axis (K-S test, $p=3.17E-16$).

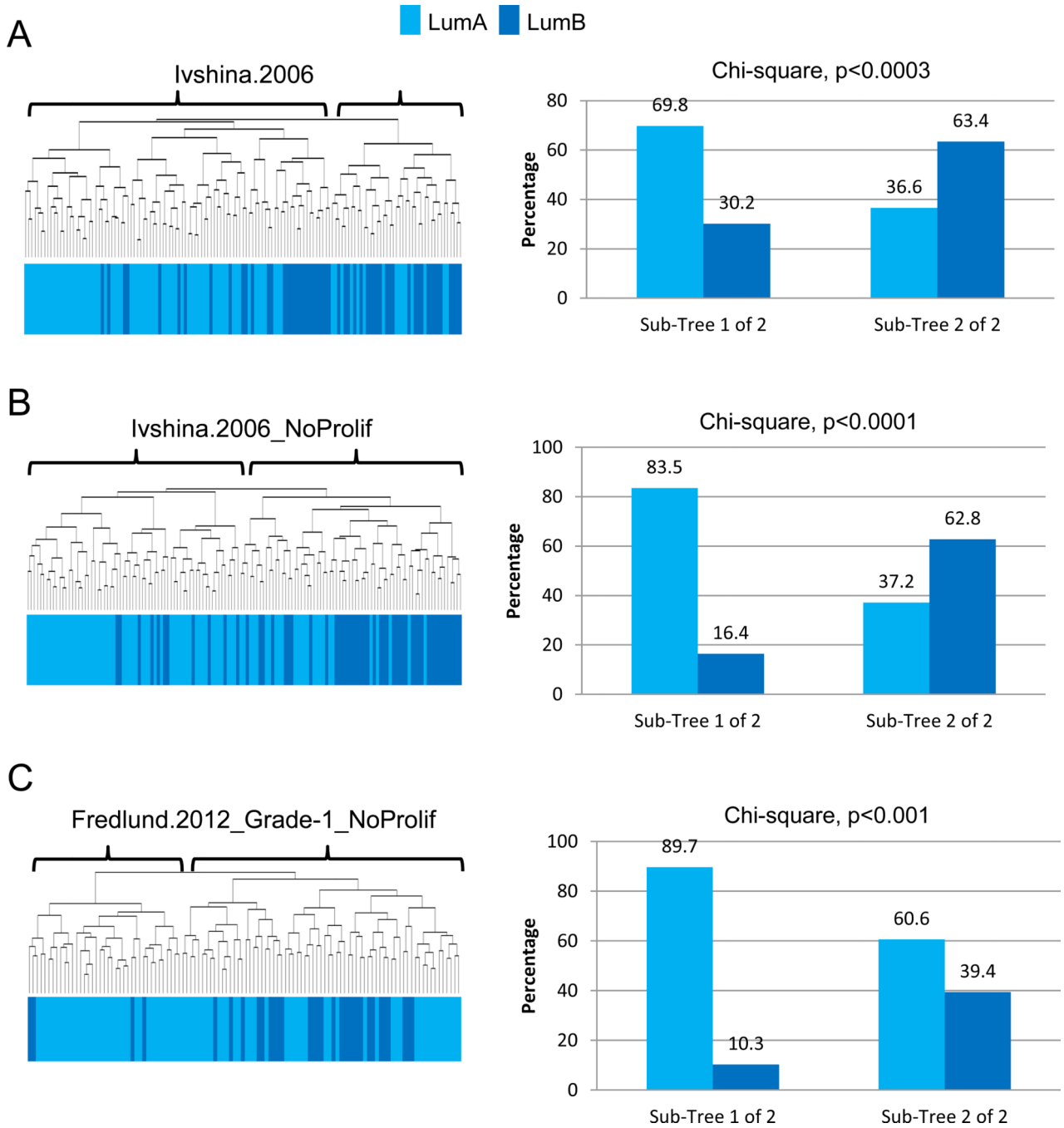


Figure 6. Luminal A and B human breast cancers are segregated by the JvA transcriptomic program

(A) Luminal A or B cancers from Ivshina et al. were clustered by the JvA 243 profile and exhibited an enrichment of luminal B cancers in the main bifurcation (30.2% in sub-tree 1 of 2; 63.4% in sub-tree 2 of 2; chi-square test, $p < 0.0003$). (B) Removal of proliferation-related genes from the JvA 243 profile did not compromise the segregation of luminal B cancers (16.4% in sub-tree 1 of 2; 62.8% in sub-tree 2 of 2; chi-square test, $p < 0.0001$). (C) Grade-1 luminal A or B breast cancers from Fredlund et al. were segregated by the JvA profile that

was divested of proliferation-related genes. The enrichment from luminal B cancers was also observed (10.3% in sub-tree 1 of 2; 39.4% in sub-tree 2 of 2; chi-square test, $p < 0.001$).